UC Irvine
UC Irvine Previously Published Works

Title
Gas emissions, minerals, and tars associated with three coal fires, Powder River Basin, USA

Permalink
https://escholarship.org/uc/item/1bm7636j

Authors
Engle, Mark A
Radke, Lawrence F
Heffern, Edward L
et al.

Publication Date
2012-03-01

DOI
10.1016/j.scitotenv.2012.01.037

Peer reviewed

Gas emissions, minerals, and tars associated with three coal fires, Powder River Basin, USA

Mark A. Engle [a,b,*], Lawrence F. Radke [c,d], Edward L. Heffern [e], Jennifer M.K. O'Keefe [f], James C. Hower [g], Charles D. Smeltzer [h], Judith M. Hower [i], Ricardo A. Olea [a], Robert J. Eatwell [d], Donald R. Blake [j], Stephen D. Emsbo-Mattingly [k], Scott A. Stout [k], Gerald Queen [l], Kerry L. Aggen [l], Allan Kolker [a], Anupma Prakash [m], Kevin R. Henke [g], Glenn B. Stracher [n], Paul A. Schroeder [o], Yomayra Román-Colón [a], Arnout ter Schure [p]

[a] U.S. Geological Survey, Reston, VA 20192, United States
[b] Department of Geological Sciences, University of Texas at El Paso, TX 79968, United States
[c] Cloud and Aerosol Research Group, University of Washington, Seattle, WA 98195, United States
[d] Airborne Research Consultants, Saunderstown, RI 02875, United States
[e] U.S. Bureau of Land Management, Cheyenne, WY 82009, United States
[f] Department of Physical Science, Morehead State University, Morehead, KY 40351, United States
[g] University of Kentucky, Center for Applied Energy Research, Lexington, KY 40511, United States
[h] School of Earth & Atmospheric Science, Georgia Institute of Technology, Atlanta, GA 30332, United States
[i] Geomed Associates, Lexington, KY 40503, United States
[j] Department of Chemistry, University of California-Irvine, Irvine, CA 92697, United States
[k] NewFields Environmental Forensics, Rockland, MA 02370, United States
[l] U.S. Bureau of Land Management, Buffalo, WY 82834, United States
[m] Geophysical Institute, University of Alaska, Fairbanks, AK 99775, United States
[n] East Georgia College, Swainsboro, GA 30401, United States
[o] Department of Geology, University of Georgia, Athens, GA 30602, United States
[p] Electric Power Research Institute, Palo Alto, CA 94304, United States

ARTICLE INFO

ABSTRACT

Ground-based surveys of three coal fires and airborne surveys of two of the fires were conducted near Sheridan, Wyoming. The fires occur in natural outcrops and in abandoned mines, all containing Paleocene-age subbituminous coals. Diffuse (carbon dioxide (CO_2) only) and vent (CO_2, carbon monoxide (CO), methane, hydrogen sulfide (H_2S), and elemental mercury) emission estimates were made for each of the fires. Additionally, gas samples were collected for volatile organic compound (VOC) analysis and showed a large range in variation between vents. The fires produce locally dangerous levels of CO, CO_2, H_2S, and benzene, among other gases. At one fire in an abandoned coal mine, trends in gas and tar composition followed a change in topography. Total CO_2 fluxes for the fires from airborne, ground-based, and rate of fire advancement estimates ranged from 0.9 to 780 mg/s/m^2 and are comparable to other coal fires worldwide. Samples of tar and coal-fire minerals collected from the mouth of vents provided insight into the behavior and formation of the coal fires.

Published by Elsevier B.V.

1. Introduction

Thousands of coal fires occur worldwide, in every major coal-bearing region and on all continents except for Antarctica (Stracher, 2010). Emissions from coal fires are a known, but poorly quantified, source of greenhouse gases; e.g. carbon dioxide (CO_2) and methane (CH_4); toxic organic compounds, e.g. benzene and hydrogen sulfide

(H_2S); volatile trace elements, e.g. mercury (Hg), arsenic, and selenium; and several other hazardous pollutants (Hower et al., 2009; O'Keefe et al., 2010). A small, but growing, body of research has been conducted to determine the composition and, in some cases, the quantity of gases generated by coal fires (Carras et al., 2009; Hower et al., 2009; O'Keefe et al., 2010, 2011; Engle et al., 2011; Ide and Orr, 2011). However, few comparisons have been made showing differences in gas composition and emissions between multiple coal fires. In addition to gas-phase products, solid and semi-solid phases (minerals and tars) form at the mouth of some coal-fire vents (Pone et al., 2007; Stracher, 2007; Silva et al., in press), but the relationship

between exhaust gas composition and mineral and tar chemistry has not been extensively studied.

Compounds found in the exhaust from coal fires, mentioned above, are similar to those found in the flue gas from coal-fired power plants, but are not subject to emission controls and technologies that minimize their release and potential impacts. The composition of the coal-fire exhaust gases has been shown to depend on the chemistry of the coal, oxygen (O_2) concentration, temperature, and physical factors such as fracturing of the overburden (Ide et al., 2010). The dominant transport mechanism for coal-fire exhaust gases includes the following: 1) convection and advection outward from gas vents and fractures; and 2) diffusion up into the soil column and eventually the atmospheric boundary layer (Engle et al., 2011). To adequately characterize emissions from a coal fire, estimates must be based on both mechanisms.

Dozens of natural and human-induced coal fires are active in the Powder River Basin (PRB) of southeast Montana and northeast Wyoming, the largest source of coal produced in the United States (Fig. 1). Coal fires exhibit surface features similar to those found above high-temperature geothermal systems including gas vents, elevated surface temperatures, expansion and subsidence related fractures, zones of dead vegetation, and geochemical alteration; i.e. clinker. The subbituminous coal beds of the Paleocene Fort Union Formation and Eocene Wasatch Formation are prone to ignition, and have burned throughout the past few million years (Reiners et al., 2011; Riihimaki et al., 2009) creating 3700 km² of reddish clinker outcrops that cap hills and ridges throughout the basin. The coal may ignite as a result of range and forest fires, lightning strikes, arson or carelessness, or spontaneous combustion. Four main types of coal fires occur: 1) fires in abandoned underground mines; 2) fires in highwalls and spoil piles in active surface mines; 3) fires on natural coal outcrops; and 4) low-level smoldering of coal beds (Heffern and Coates, 2004). Scientists with the U.S. Bureau of Land Management (BLM) have documented 81 known historic and active coal fires in the PRB in abandoned mines, natural outcrops, and spoil piles.

This article presents quantitative and qualitative assessments of gaseous emissions and qualitative examinations of related mineral and tar phases produced by three coal fires in the PRB, using results from a 11–15 May 2009 field campaign that included ground- and aerial-based surveys of three coal fires located roughly 16 km north of Sheridan, Wyoming. The details concerning CO_2 and CH_4 emission estimates and comparison of ground-based and airborne methods for the Welch Ranch site were discussed in detail by Engle et al. (2011). Results from that work show that the two methods gave emissions estimates that agree within a factor of two: the total CO_2 emitted from the soil and vents was 6.8–9.0 t CO_2/d and 19–25 kg CH_4/d using the ground-based approach compared with airborne estimates of 3.5–4.1 t CO_2/d and 11–13 kg CH_4/d.

2. Description of the coal fires

The three fires examined in this paper occur along a southwest-to-northeast trend near the banks of the Tongue River in north-central Wyoming and have distinct geomorphic features (Fig. 1). The most northern fire investigated, the Ankney fire, occurs in a natural outcrop along the cut bank of the river and is of unknown origin but thought to have started circa 1990. The fire primarily consumes the Anderson coal bed and no attempt has been made to extinguish it. The surface expression of the Ankney fire is a series of arcuate fractures associated with the slumping/collapse of the surface that lay above voids left by the burned-out coal (Fig. 2). The fire is marked by the absence of vegetation in the most active areas, a consequence of the heat at the surface. A map of the burned-out area at the Ankney site (Fig. 3) shows that the fire front, as represented by fractures, has advanced to the southeast at an average rate of 6 m/yr over the past 7 years. Measurements by the BLM show that the fire-impacted area increased from 0.6 ha in May 2004 to 1.4 ha in September 2011 (Fig. 3).

The two southern fires, the Welch Ranch and Hotchkiss fires, have been burning in the Monarch coal (and Dietz 2 and 3 for the Welch Ranch fire) since the early to mid 1900s and are likely related to underground coal mining. The Acme mine, the northern edge of which is on the Welch Ranch now owned by BLM, operated from 1911 through 1940 (Fig. 1). Total disturbance from the mine includes >200 ha of underground operations (Dunrud and Osterwald, 1980), which eventually subsided. As the rooms between pillars collapsed, sinkholes allowed O_2-rich air to enter. Coal-bed fires sporadically ignite in those sinkholes, producing many of the coal fires in this region. The 4.7-ha Hotchkiss fire exhibited limited surface expression during the field campaign, and is constrained to a few active vents.
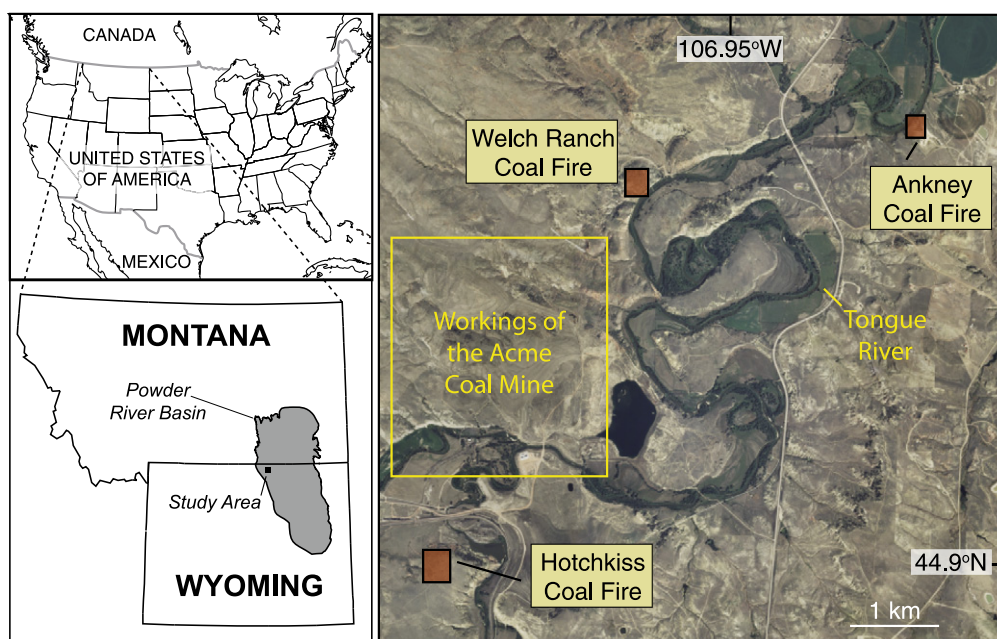

Fig. 1. Maps indicating location of study area and annotated aerial photograph noting locations of the coal fires and other major features. Airborne imagery collected in 2009 by the U.S. Department of Agriculture.

Fig. 2. A) Photograph of arcuate fractures in developing part of Ankney fire. The most intense part of the fire, generally towards the lower right corner of the picture, has not yet undermined this area, but subsidence related to the fire-related removal of the coal has begun. B) Photograph of the Ankney fire. Soil CO_2 flux measurements in foreground; measuring in situ gas composition, and collection of volatile organic gas samples in the background. The most intense part of the fire is to the left of the picture.

Conversely, the 1.7-ha Welch Ranch, like the Ankney fire, exhibited a chain of active vents and unvegetated patches and linear-to-arcuate fractures that vent the coal-fire gases. While there are barren areas associated with the Welch Ranch fire, much of the surface is vegetated and is used for livestock grazing. In September 2002, Wyoming's Abandoned Mine Lands Division attempted to extinguish the Welch Ranch by injecting a sandy slurry into fissures along the north edge of the fire and bulldozing the fissures shut (Murja, 2002; Heffern et al., 2003). This intervention slowed the advance but did not extinguish the fire, which continues to burn. A second round of reclamation is being considered.

2.1. Coal quality

Fresh coal samples were not accessible at any of the coal fire sites, so published coal quality data from the region were used. Averages of all samples for the Acme 7 1/2-minute quadrangle, the location of all of our study sites, indicate that the coals generally have high moisture and low heating values, typical of subbituminous coals (Table 1). The major oxides and minor element concentrations and the generally low sulfur content of the coal samples have implications for the species of neoformed minerals precipitated at the vents.
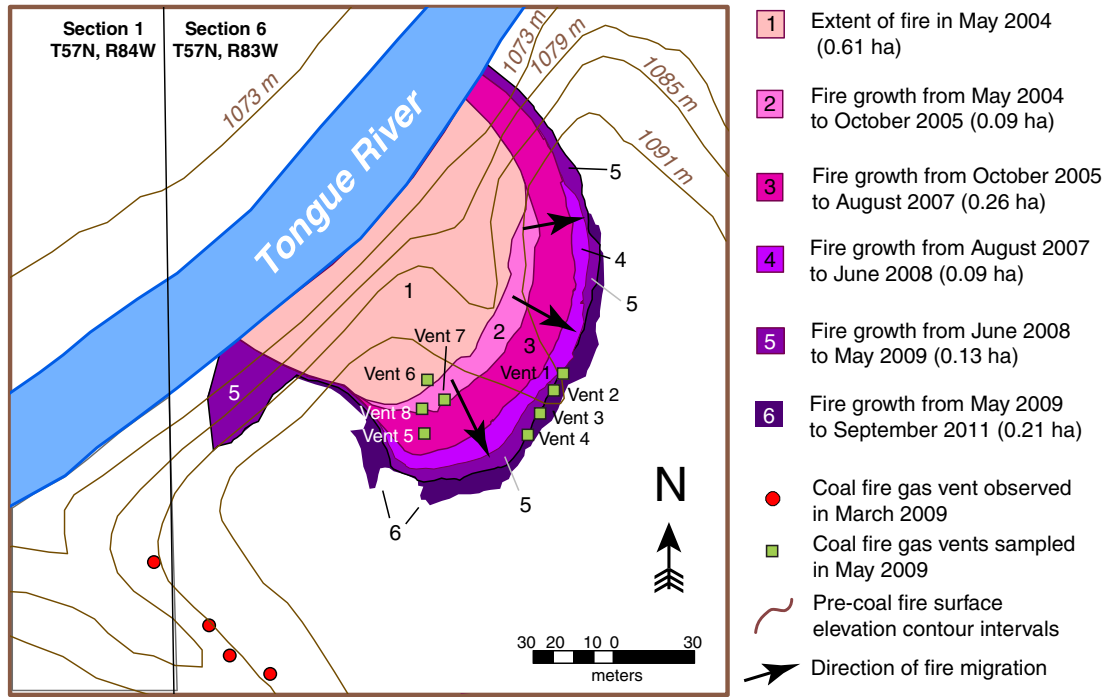
Fig. 3. Advances of the Ankney fire from May 2004 to September 2011, as determined by ground-based GPS surveys.

3. Methods

The field procedure employed three teams: two on the ground responsible for diffuse CO_2 flux determination (Section 3.1), gas flow and chemistry (Section 3.2) and mineral and tar collection (Section 3.3); and one team in an airplane (Section 3.4). In addition, coal consumption estimates were calculated at the Ankney fire using the apparent rate of fire advancement based on multiple BLM land surveys (Fig. 3).

3.1. Diffuse CO_2 emissions

Point measurements of diffuse fluxes of CO_2 were performed using standard accumulation chamber techniques (Bergfeld et al., 2006) and a USGS-designed flux system described in Engle et al. (2011). The method consists of measuring the rate of CO_2 accumulation in the chamber ($\partial C/\partial t$) after the chamber is sealed to the ground surface; the soil flux (F) of CO_2 (g/m²d) is calculated as follows:

$$F = \left[\frac{\rho V}{A} \frac{\partial C}{\partial t}\right], \tag{1}$$

where ρ is gas density, V is the flux system volume, A is the footprint of the flux chamber, and $\partial C/\partial t$ is the CO_2 accumulation rate in the chamber. To examine for repeatability and small-scale heterogeneity, diffuse soil fluxes were measured at three locations within a 1-m

radius at roughly 10% of the points (n = 15). Relative standard deviations from the three measurements ranged from 16 to 132% with a median of 48%. At each soil CO_2 flux point, soil temperature was measured at the surface using an infrared (IR) thermometer and at 10-cm depth using a K-type thermocouple immediately before or after each flux measurement.

Soil CO_2 flux points for the Welch Ranch and Hotchkiss coal fires were arranged in a N–S/E–W grid with additional measurement sites added in and around thermal anomalies within the grid (Fig. 4). For the Ankney fire, safety and access issues prevented layout of a grid, so CO_2 flux points were placed as equidistant as possible (Fig. 4). To estimate total diffuse CO_2 emissions for each study area, the CO_2 flux data were interpolated using sequential Gaussian simulation (SGS). For interpolation calculations, negative fluxes (these can result from input of soil gas with a lower CO_2 concentration than that of the air originally in the chamber) and $\partial C/\partial t$ measurements not significantly different than zero ($p < 0.05$) were assigned a value equal to the method detection limit. The application of SGS to diffuse CO_2 emissions from coal fires is detailed in Engle et al. (in press). Briefly, a semivariogram model is developed for each fire based on Box–Cox transformed CO_2 flux data. This model is then used to generate 100 realizations of diffuse CO_2 flux for each fire, which are back-transformed into the original units. Integrating CO_2 fluxes across each site generates a histogram of total CO_2 emissions for that fire. The SGS modeling, variogram modeling, and integration were completed using SGemS 2.1 (Remy et al., 2009). Because

Table 1
As-received coal quality and chemistry data for unweathered coal samples from the Acme 7 1/2-minute quadrangle. Mois = moisture; VM = volatile matter; FC = fixed carbon. Data taken from Bragg et al. (1997) and unpublished data from the U.S. Bureau of Mines BMALYT dataset.

	Heating value		Mois	VM	FC	Ash	H	C	N	O	S_{total}	Hg
	BTU	MJ/kg	%	%	%	%	%	%	%	%	%	mg/kg
Avg.	9780	22.8	20.5	32.7	42.4	4.3	6.2	56.1	1.07	31.1	0.47	0.09
Std. dev.	265	0.62	1.7	1.8	2.9	0.9	0.1	1.0	0.06	0.5	0.21	0.05
Max.	10,100	23.5	23.4	36.8	47.2	6.0	6.2	56.8	1.10	31.4	1.16	0.20
Min.	9130	21.2	18.1	30.3	35.9	3.11	6.1	55.0	1.00	30.5	0.25	0.04
Number	17	17	17	17	17	17	3	3	3	3	17	9
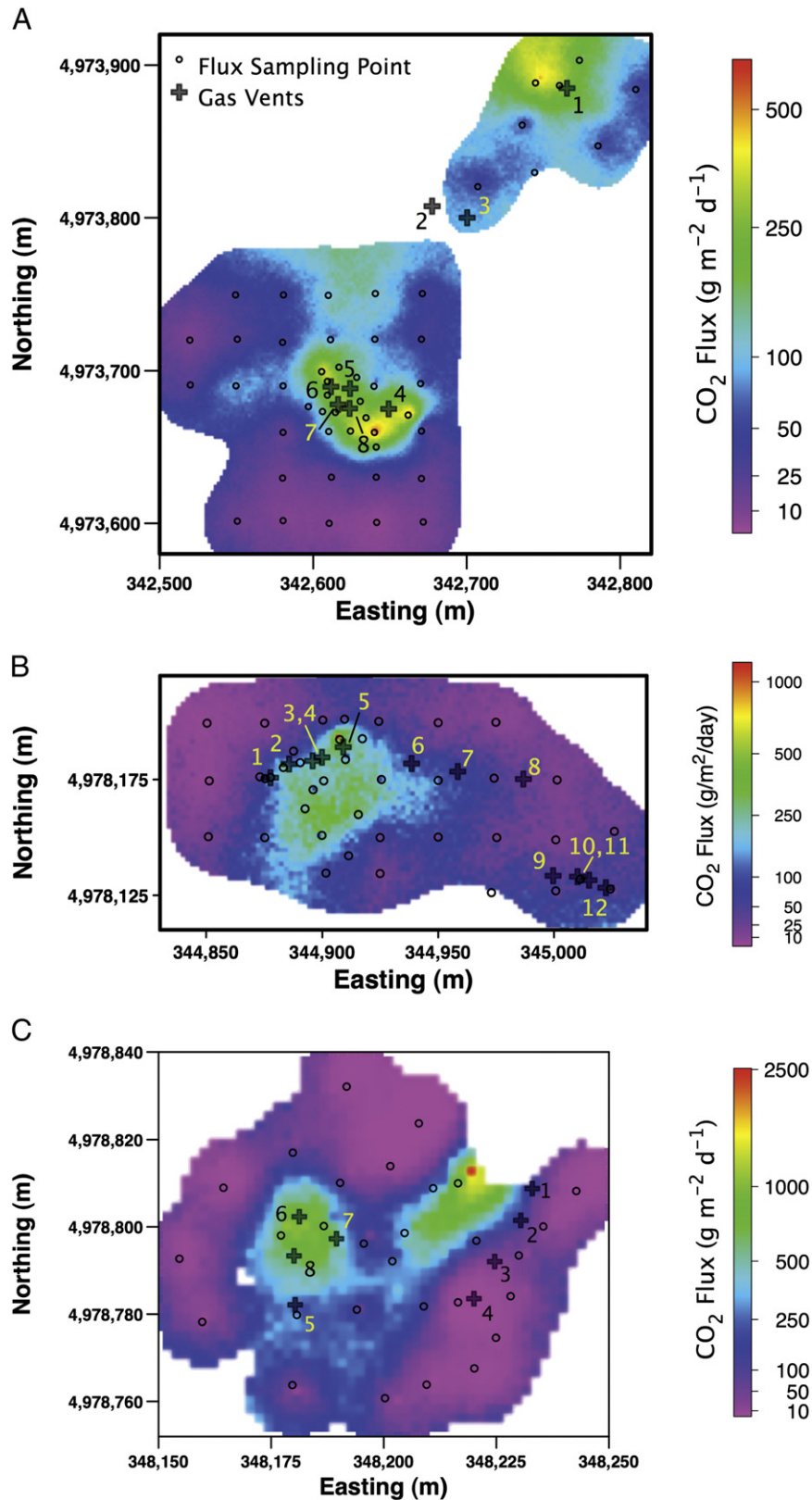
Fig. 4. False color heat maps of the diffuse CO_2 fluxes determined from nodal means (see text) for the (A) Hotchkiss coal fire, (B) Welch Ranch coal fire, and (C) Ankney coal fire. Vent numbers on each map correspond with those found in Table 2. (For interpretation of the references to color in this figure legend, the reader is referred to the web version of this article.)

measurement of background CO_2 emissions was not possible, it was estimated from median CO_2 flux for the lowest subpopulation observed in quartile-normality plots. The background estimates for each fire were subtracted from SGS-calculated emissions.

3.2. Composition of coal-fire gases and calculation of vent emissions

Concentrations of gases in active exhaust vents were determined both in near-real time, using in situ analyzers, and post sampling,

from laboratory analyses of collected samples (Fig. 5). At each vent, concentration data for the individual compounds are combined with the corresponding gas flow data to determine vent emissions such that:

$$E_i = C_i VA, \tag{2}$$

where E_i is the emission of gas component i, C_i is the concentration of component i in the vent, V is the velocity of the gas perpendicular to the vent (assuming the velocity is equivalent for each gas component), and A is the cross-sectional area of the vent at the surface (O'Keefe et al., 2010). Vent-gas velocities were determined using an S-type Pitot tube in conjunction with a Flow Kinetics FKT 1 1DP1A-SV flow meter (O'Keefe et al., 2010). The range of velocities measured in the vents (0.5–4.26 m/s) is within the limitations of the flowmeter/Pitot tube setup (0.5–12.9 m/s). Often large vents (>100 cm^2) were broken into smaller subsections, measured individually, and emissions were summed across the entire vent.

Vent-gases were analyzed in situ for CO_2, CO, CH_4, H_2S, and Hg. The first four constituents were measured using an Industrial Scientific MX6 iBrid portable gas analyzer. The gas analyzer was calibrated with zero and span standards before and after each field campaign; no marked drifts were observed. Measurement accuracy for the iBrid instrument ranges from ± 2–10% depending on the gas and concentration range. Mercury concentrations were measured with a differential Zeeman atomic absorption spectrometry Ohio Lumex RX-915 Portable Mercury Analyzer. The Lumex analyzer was calibrated at least once a day using an internal calibration cell; measurement accuracy for the Lumex is ± 5-20%, depending on the concentration range. Within each vent (or each section of a vent) in situ gas measurements were made at a minimum of five locations.

Volatile organic compound (VOC) gas samples were collected in electropolished, stainless steel, evacuated canisters. The samples were analyzed for a suite of carbon-bearing gases (i.e., CO, CO_2, carbonyl sulfide, dimethylsulfide, and carbon disulfide), C1-to-C9 aliphatic compounds, and single-ring aromatics (benzene, toluene, ethylbenzene, and xylene) on a gas chromatographic system in the Rowland-Blake Group laboratory at the University of California-Irvine. Analytical methods are described in Barletta et al. (2008) following quality assurance/quality control protocols of Colman et al. (2001). Previous use of these techniques to produce VOC analyses of coal-fire exhaust gases is provided in Stracher et al. (2006) and Hower et al. (2009).

3.3. Coal-fire minerals and tars

Minerals and tar frequently deposit on the mouth of coal-fire vents, and are formed through isochemical and mass-transfer processes (Stracher, 2007). Samples were collected from each fire; the minerals were identified using X-ray diffraction (XRD), and the tars were characterized using organic analyses. Powder XRD analyses of the mineral samples were performed at the University of Georgia with a Bruker D8 Advance diffractometer using co-radiation at 40 mA and 40 kV with a step size of 0.01° 2Q and a scan rate of 2.5° per minute, with a Lynx-eye® 192 position sensitive detector. The samples were dry mounted in aluminum holders and scanned at 8–60° 2θ with Cu K_α radiation.

Tar samples were analyzed using gas chromatography/flame ionization detection (GC/FID) at NewFields Environmental Forensics to measure C9-C44 hydrocarbons (Environmental Protection Agency (EPA) Method 8015) and gas chromatography/mass spectrometry (GC/MS) using a modification of EPA Method 8270C to identify Polycyclic Aromatic Hydrocarbons (PAHs) with 2 to 7 rings, including parent and alkylated isomers and geochemical biomarkers (Stout and Emsbo-Mattingly, 2008).

3.4. Remote sensing

Airborne remote sensing of the coal fires was conducted with a Cessna 337 Super Skymaster (owned and operated by Airborne Research Consultants, Saunderstown, Rhode Island) equipped with a FLIR™ A320 camera, a non-contact thermal device operating in the spectral range of 7.5 to 13 μm, mounted under the aircraft wing for

Fig. 5. Photograph of two ground teams at work along linear vent structure at Welch Ranch fire. The team on the left is measuring in situ gas composition, and collection of volatile organic gas samples. The team on the right is conducting the diffuse soil CO_2 flux measurements.

the pre-dawn flights.[1] The camera has an instantaneous field of view (FOV) of 25° and provides 16-bit images at an accuracy of ±0.2 °C or ±2%. The altitude of the aircraft was maintained at ~2900 m above mean sea level (MSL) compared with the ground elevation for the fire sites of ~1130 m MSL, yielding a pixel size of about 2.5×2.5 m. The FLIR™ software directly recorded surface kinetic temperature images by using modified MODTRAN code to perform atmospheric correction of the thermal data, based on local atmospheric conditions such as the target temperature, air temperature, and air density.

Data processing of the IR imagery to estimate energy emissions from the fire was focused on decomposing the data based on the dominant Gaussian features. An automated program was developed to detect fire-related thermal anomalies and determine corresponding boundaries for calculating the total energy for each fire. First, the program computes a temperature frequency distribution for the IR image which, in turn, is broken down by each local minimum as function of temperature. A Gaussian distribution is fit to each segment, giving standard deviation and other statistical properties. The segment with highest frequency amplitude is assumed to be the land segment. The second highest frequency distribution is assumed to be surface water, e.g. the Tongue River, if the standard deviation of that segment is significantly smaller, i.e. thermally monotonous, than that for the land segment. The remaining segments are assumed to be fire anomalies and are integrated to give the total fire energy emission. Each segment is assigned a numerical identity corresponding to land, water, or fire anomaly, allowing heat flux to be calculated from data for individual frames. The CO_2 emissions were estimated from the heat emission data through application of the Stefan–Boltzman law for gray bodies (Engle et al., 2011); and the heating value and carbon content of the coals in the region, taken from published literature (Table 1). Estimation of the coal-consumption rate allows for calculation of CO_2 emissions (Engle et al., 2011).

4. Results

4.1. Diffuse CO_2 emissions

A total of 153 diffuse CO_2 flux measurements were made at 119 sampling points across the three coal fires. Fig. 4 shows the location of the sampling points on maps that show nodal means from the 100 SGSs of the CO_2 flux data for the three fires. Individual CO_2 fluxes ranged from −42 to 29,500 g/m²/d (negative fluxes can result from input of soil gas with a lower CO_2 concentration than that of the air in the chamber at the start of the measurement). Multiple comparisons after a Kruskal–Wallis test indicate that median diffuse CO_2 fluxes were significantly greater ($p<0.05$) for the Hotchkiss coal fire (median = 71.2 g/m²/d) relative to the Welch Ranch (median = 25.2 g/m²/d) and Ankney (median = 10.3 g/m²/d) coal fires. However, maximum diffuse CO_2 fluxes were much greater at the Welch Ranch and Ankney coal fires relative to the Hotchkiss coal fire (29,500, 2460, and 757 g/m²/d, respectively) indicating that the flux data from the former fires exhibit more highly skewed distributions (Fig. 6). For comparison, median background fluxes were 8.3, 4.4, and 1.7 g CO_2/m²/d for the Hotchkiss, Welch Ranch, and Ankney coal fires, respectively; these estimates of background fluxes are typical for expected soil CO_2 fluxes given the climatic conditions of the Powder River Basin (<10 g CO_2/m²/d; Raich and Potter, 1995). Correlations between soil temperature (at 10-cm depth) and diffuse CO_2 fluxes are positive, varied (Spearman $\rho = 0.69–0.90$), and statistically significant for all three fires ($p<0.01$). Significant relationships were also found between soil temperatures and diffuse gas fluxes for coal fires in Australia and Alabama (Carras
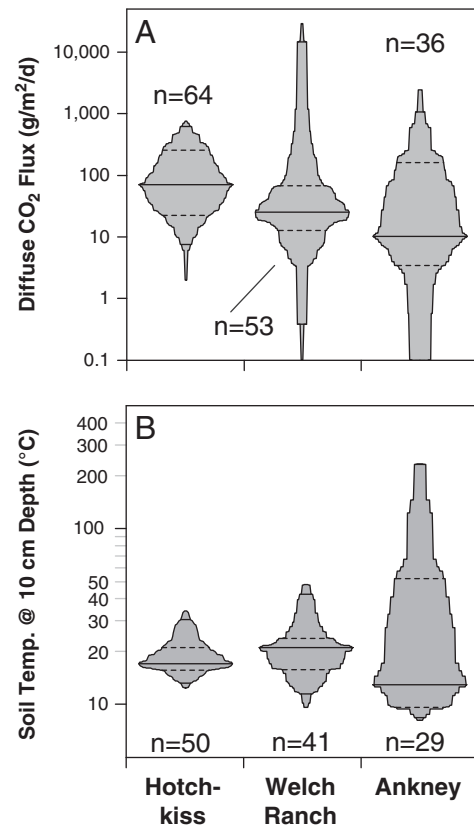
Fig. 6. Box-percentile plots showing distribution of diffuse CO_2 flux measurements (A) and soil temperatures at a depth of 10 cm (B) for the Hotchkiss, Welch Ranch, and Ankney coal fires. For plotting purposes, CO_2 fluxes <0.1 g/m²/d were truncated. Solid horizontal line indicates sample median and dashed horizontal lines demarcate 1st and 3rd quartiles.

et al., 2009; Engle et al., in press). Integration of the SGS results provides background-corrected diffuse CO_2 emission estimates of 4.0 ± 0.48, 1.2 ± 0.2, and 0.91 ± 0.24 t/d for the Hotchkiss, Welch Ranch, and Ankney fires, respectively. The estimate for Ankney is considered a minimum value given the scarcity of data for active portions of the fire.

4.2. Composition of coal-fire gases and vent emission rates

In situ measurements of the composition of coal fire vent gases and emission rates were conducted at 12 vents at Welch Ranch and nine vents at Ankney (Tables 2, 3; Fig. 4). Additional vents at the Ankney fire were observed but were not sampled due to safety considerations. In situ gas chemistry was determined at the eight vents at the Hotchkiss fire (Table 2), but problems with velocity measurements prevented calculation of emission rates. Carbon dioxide was the dominant gas measured in the exhaust from the three fires. Although the highest exhaust gas temperatures were observed in vents at the Ankney fire (up to 319 °C), higher CO_2 concentrations (up to 3.06%) were measured at the other two fires. Post Kruskal-Wallis multiple comparison tests show that median CO_2 concentrations were greater (at $p<0.01$) in exhaust from the Hotchkiss fire than for the other fires. Carbon monoxide, CH_4, and H_2S concentrations were detectable at roughly half of the vents, indicating large spatial variability in combustion behavior. Mercury concentrations in gas vents ranged by nearly four orders of magnitude from 15 ng/m³ (roughly ten times ambient air) to concentrations more typical of fumarolic vents (up to 12,100 ng/m³; cf. Engle et al., 2006). The large range in Hg concentrations in vent gas can be attributed to the heterogeneity

Table 2
Vent area, flow, temperature, and in situ gas chemistry for coal-fire exhaust gas at the Hotchkiss, Welch Ranch, and Ankney sites. <dl = less than method detection limit.

Vent[a]	Vent area (m^2)	Velocity (m/s)	Velocity std. dev. (m/s)	Temp. (°C)	Flow-averaged concentrations					
					CO_2 (%)	CO (ppmv)	CH_4 (%)	H_2S (ppmv)	CO_2/CO (molar ratio)	Hg (ng/m^3)
Hotchkiss Fire										
1	–	–	–	34.6	1.01	<dl	<dl	<dl	–	22
2	–	–	–	18.1	2.13	<dl	<dl	<dl	–	16
3	–	–	–	27.0	3.06	<dl	<dl	<dl	–	35
4	–	–	–	27.9	1.3	<dl	<dl	<dl	–	40
5	–	–	–	42.9	1.55	<dl	<dl	<dl	–	57
6	–	–	–	43.9	1.71	<dl	<dl	<dl	–	71
7	–	–	–	45.9	1.87	<dl	<dl	<dl	–	104
8	–	–	–	44.0	1.48	<dl	<dl	<dl	–	118
Welch Ranch Fire										
1	1.618	1.92	0.73	26.6	0.96	<dl	<dl	<dl	–	500
2	0.484	2.27	0.78	39.4	0.26	<dl	<dl	<dl	–	714
3	0.282	2.07	1.01	45.5	1.31	<dl	<dl	<dl	–	483
4	0.173	2.37	0.71	37.3	1.13	<dl	<dl	<dl	–	836
5	0.016	1.47	0.63	36.8	1.20	<dl	<dl	<dl	–	204
6	0.012	1.98	0.34	48.3	1.22	<dl	<dl	<dl	–	321
7	0.049	2.02	0.34	15.6	0.81	<dl	<dl	<dl	–	47
7-2	0.049	0.82	0.15	26.3	1.06	31	<dl	2.5	218	116
8	0.002	2.61	0.30	17.6	0.81	<dl	<dl	<dl	–	–
8-2	0.002	1.30	0.32	28.7	1.17	<dl	<dl	2.1	–	15
9	0.160	3.66	0.25	17.2	0.36	41	<dl	<dl	56	–
9-2	0.160	0.60	0.21	26.3	0.91	36	<dl	2.0	161	321
10	0.675	1.16	0.25	48.1	1.07	553	0.13	2.3	12	–
10-2	0.135	0.98	0.21	47.5	0.94	298	<dl	2.8	20	478
11A	0.080	1.46	0.24	54.1	1.19	764	0.17	3.1	10	–
11B	0.025	0.84	0.14	45.5	1.19	759	0.19	2.9	10	–
11A-2	0.080	1.17	0.21	54.4	0.88	29	<dl	2.6	193	383
11B-2	0.025	1.50	0.33	57.2	0.82	240	<dl	2.4	22	303
12B	0.019	1.81	0.94	38.3	1.26	528	0.13	2.3	15	–
12-2	0.019	1.19	0.46	43.1	1.14	301	<dl	2.4	24	276
Ankney Fire										
1	0.360	2.24	0.19	9.9	0.12	162	<dl	<dl	4.8	113
2	0.971	2.41	0.14	16.0	0.15	82	<dl	0.66	11	84
3	0.027	0.78	0.20	19.1	0.36	498	0.33	6.4	4.6	402
4	0.027	0.96	0.32	23.7	0.08	674	0.44	10.4	0.8	242
5	0.023	1.43	0.86	82.2	1.90	3710	0.60	94	3.3	3950
6	0.056	4.26	0.78	195	1.87	123	<dl	3.3	96.8	1200
7	0.080	3.00	0.78	319	1.51	45	<dl	5.6	213.6	12,100
8	0.048	1.70	0.39	51.6	1.09	1460	<dl	62.8	4.8	559
9	0.126	0.50	0.22	101	0.89	1440	0.25	9.1	3.9	1080

Notes:
[a] Exhaust gases in vents with a "-2" suffix were remeasured on May 14, 2007 (1 day after the original survey), due to incomplete Hg data for the original survey.

of Hg concentrations in the coal (Table 1), relatively low concentrations of Hg in ambient air, and large ranges in temperature across the fires (Table 2). Multiple comparisons after a Kruskal–Wallis test indicate that median Hg concentrations were higher in exhaust gases at the Ankney fire than for the other fires ($p < 0.01$).

Vents at the Welch Ranch fire were emitting about 3.8 t CO_2/d and 130 mg Hg/d; roughly 50% of the total emission for both gases was emanating from the largest vent (Vent 1 area = 1.6 m^2). Notably, CO_2 and Hg concentrations measured in this vent were typical of those for other vents, demonstrating the potential effect of vent area on total emission estimates. Conversely, H_2S and CO emissions were greatest from vents 9–12, suggesting a variation in spatial control on vent chemistry at the site.

Emissions and concentrations of CO_2, CO, CH_4, and H_2S in exhaust gases from Welch Ranch vents 7–12 were measured twice during the campaign, once on 13 May 2009 and again on 15 May 2009. Results from Wilcoxon signed-rank tests for paired data indicate that median CO_2 emissions were significantly lower ($p < 0.05$; 51% lower, on average) on the second sampling day relative to the first, but that emissions for CO and H_2S did not significantly differ ($p > 0.05$) between days. These findings indicate that temporal variations in concentrations and fluxes can be large, even over small, daily timescales.

Due to the incomplete coverage of presumably high emission sites at the Ankney fire, discussions of average emission rates and comparisons of the Ankney and Welch fire are negatively biased. Given that context, total vent CO_2 emissions from Welch Ranch were about three times higher than those at Ankney. However, most of the measured parameters, including vent temperatures (up to 319 °C), gas concentrations and vent emissions of CH_4, H_2S, and Hg were higher for the Ankney fire than for the Welch Ranch fire (Tables 2, 3). Mercury concentrations in Ankney vents (up to 12,100 ng/m^3) were particularly elevated and emissions from a single vent of up to 250 mg/d demonstrate that coal fires may be an important source of atmospheric Hg.

Volatile organic carbon content of vent exhaust was determined from samples at two vents each at the Hotchkiss and Welch Ranch fires and four vents at the Ankney fire (Table 4). The VOCs show distinct differences between and within sites. Gas samples from vent 10 at Welch Ranch and vents 3 and 9 at the Ankney fire are notable for their elevated benzene concentrations (up to 3.8 ppmv) and also exhibit elevated concentrations of several aliphatic compounds (up to 0.7% CH_4 and 18.1 ppmv C_2H_6), indicating incomplete combustion of the coal. Conversely, samples from vent 1 at the Welch Ranch fire, vent 5 at the Hotchkiss fire, and vent 6 at Ankney exhibit much lower ratios of CO to CO_2 (except for the latter vent),

Table 3
Vent emission data for coal-fire exhaust gas at the Welch Ranch and Ankney sites.

Vent[a]	Vent emissions				
	CO_2 (kg/d)	CO (kg/d)	CH_4 (kg/d)	H_2S (g/d)	Hg (mg/d)
Welch Ranch Fire					
1	3800 ± 810	<dl	<dl	<dl	130 ± 35
2	380 ± 93	<dl	<dl	<dl	68 ± 11
3	960 ± 200	<dl	<dl	<dl	24 ± 3.9
4	590 ± 96	<dl	<dl	<dl	30 ± 4.6
5	37 ± 9.9	<dl	<dl	<dl	0.42 ± 0.12
6	35 ± 6.4	<dl	<dl	<dl	0.64 ± 0.11
7	110 ± 19	<dl	<dl	<dl	0.40 ± 0.018
7-2	57 ± 10	0.11 ± 0.019	<dl	10 ± 1.9	0.40 ± 0.074
8	4.7 ± 0.55	<dl	<dl	<dl	–
8-2	3.2 ± 0.16	<dl	<dl	0.45 ± 0.11	0.0027 ± 0.00066
9	290 ± 20	2.1 ± 0.14	<dl	<dl	–
9-2	120 ± 41	0.29 ± 0.10	<dl	20 ± 7	2.7 ± 0.93
10	210 ± 46	6.9 ± 1.5	9.4 ± 2.2	35 ± 7.4	–
10-2	160 ± 33	3.1 ± 0.66	<dl	36 ± 7.5	5.5 ± 1.1
11A	170 ± 29	7.0 ± 1.2	9 ± 1.5	35 ± 5.8	–
11B	32 ± 5.4	1.3 ± 0.22	1.8 ± 0.32	6 ± 1	–
11A-2	100 ± 18	0.21 ± 0.039	<dl	23 ± 4.2	3.1 ± 0.56
11B-2	37 ± 8.2	0.70 ± 0.15	<dl	8.5 ± 1.9	0.98 ± 0.22
12B	57 ± 19	1.5 ± 0.50	2.2 ± 0.73	8 ± 2.6	–
12-2	33 ± 8.4	0.56 ± 0.14	<dl	5.4 ± 1.4	0.46 ± 0.12
Total[b]	6700 ± 850	19 ± 2.0	22 ± 2.8	84 ± 9.9	270 ± 37
Ankney Fire					
1	140 ± 7.3	12 ± 0.48	<dl	<dl	7.9 ± 0.32
2	480 ± 35	17 ± 1.9	<dl	160 ± 0.030	17 ± 0.49
3	10 ± 1.2	0.92 ± 0.23	3.5 ± 0.11	14 ± 0.0017	0.73 ± 0.086
4	2.8 ± 0.45	1.5 ± 0.24	5.6 ± 0.9	28 ± 0.0045	0.54 ± 0.086
5	70 ± 27	8.7 ± 3.4	8.0 ± 3.1	270 ± 0.10	11 ± 4.3
6	380 ± 34	1.6 ± 0.14	<dl	51 ± 0.0047	25 ± 2.1
7	250 ± 65	0.47 ± 0.12	<dl	71 ± 0.019	250 ± 66
8	110 ± 25	9.4 ± 2.2	<dl	490 ± 0.11	3.9 ± 0.91
9	120 ± 23	12 ± 2.2	12 ± 2.7	96 ± 0.016	5.9 ± 2.6
Total	1600 ± 92	64 ± 5.0	29 ± 4.2	1200 ± 0.16	320 ± 66

Notes:
 [a] Exhaust gases in vents with a "-B" suffix were remeasured on May 15, 2007 (2 days after the original survey), due to incomplete Hg data for the original survey.
 [b] This is a sum of the original survey data, except for Hg which includes a mix of data from both surveys.

lower abundances of aliphatics, and benzene concentrations below 0.007 ppmv, suggesting more complete combustion of the source coal for these vents.

4.3. Composition of minerals and tars

Only one of the 2009 samples (collected near Welch Vent 12-B) contained high-temperature minerals in a quantifiable amount. The sample was a white crust recovered from a red, altered soil adjacent to the vent. X-ray diffraction analysis identified the presence of potentially coal-fire related minerals: cordierite ($[Mg,Fe]_2Al_4Si_5O_{18}$), osumilite ($[K,Na][Mg,Fe]_2[Al,Fe]_3[Si,Al]_{12}O_{30} \cdot H_2O$), and, possibly, cristobalite (higher temperature SiO_2 polymorph). Minerals commonly found in soils and clastic sediments were also detected and include: hematite, quartz, calcite, and plagioclase. Although cordierite, osumilite, and cristobalite could have originated from the coal fires, they could also weather and erode from regional outcrops of unrelated clinker, volcanics, and contact metamorphic rocks. Apparent encrustations of minerals at Ankney were in the part of the fire in proximity to extreme heat and dangerous gases and were inaccessible.

Previous solid phase samples at the Welch Ranch fire were collected in 2004 (G. B. Stracher, unpub. data). At that time, ground subsidence, fissures, gas vents, outcrops of porcellanite (red and green baked and fused shale) and red, baked sandstone in association with both active and formerly active areas of burning coal were observed. At several active-burn sites, surficial hot spots or gas vents were encrusted with

gypsum, tschermagite ($NH_4AlSO_4 \cdot 12H_2O$), quartz, and cristobalite (Table 5). Additional details about the mineralogy of coal-fire related minerals can be found elsewhere (Pone et al., 2007; Stracher, 2007; Silva et al., in press).

In 2009, eight samples of tar were collected from the mouth of vents at the Hotchkiss and Welch Ranch fires. The concentration of total extractable petroleum hydrocarbons (TEH) eluting between *n*-nonane (*n*-C_9) and *n*-tetratetracontane (*n*-C_{44}) ranged from 54,600 to 216,000 mg/kg in four Hotchkiss samples and 89,500 to 1,000,000 mg/kg in the four Welch samples (Table 6). Most of this mass consisted of large hydrocarbons and carbon molecules with masses in excess of *n*-C_{44} (e.g., soot). The sum of the 16 EPA priority pollutant PAH concentrations ranged from 31.5 to 157 mg/kg in the samples from the Hotchkiss fire and 53.6 to 438 mg/kg in the samples from the Welch Ranch fire. These results indicate that the Hotchkiss fire generated slightly lower hydrocarbon and PAH concentrations compared with the Welch Ranch fire, possibly as a consequence of more complete combustion.

High proportions of parent compounds relative to alkylated PAHs indicate that PAHs in the tars were pyrogenic in origin (Yunker et al., 2002). Geochemical biomarkers (i.e., sesquiterpanes, triterpanes, steranes, and triaromatic steranes) were not detected. The EPA priority PAHs generally comprised less than 0.060% of the TEH with elevated concentration in some samples from both the Hotchkiss (up to 0.074%) and Welch Ranch fires (up to 0.154%) (Table 6). The source ratio of fluoranthene relative to pyrene (FL0/PY0) ranged from 0.81 to 1.04 with little to no distinction in samples between the two fires (Table 6). These ratios of FL0/PY0 are similar to those for industrial tars carbonized from petroleum (Stout and Emsbo-Mattingly, 2008). Once exposed to the surface environment, lighter PAHs weather more rapidly than heavier PAHs; this relationship is quantified using the Pyrogenic Weathering Index (PWI) (Uhler and Emsbo-Mattingly, 2006). The estimated PWI for the samples indicates that the coal tars are lightly to moderately weathered (Table 6) and it is evidence the PAHs may be mobile in the environment.

The saturated aliphatic compounds in the samples represent coal distillates from the original subbituminous coal that avoided carbonization due to non-uniform heating during combustion (Fig. 7). Patterns of these saturated aliphatics exhibit several common features. The concentrations of heavy normal alkanes with odd carbon numbers eluting *n*-tricosane (*n*-C_{23}) to *n*-pentatriacontane (*n*-C_{35}) are markedly greater than the even carbon numbers. This pattern is indicative of a source of cuticular waxes from leaves and trees (Simoneit, 1984). Another common terrigenous feature is the high proportion of pristane (Pr) relative to phytane (Ph). By contrast, the variable proportions of isoprenoid hydrocarbons relative to normal alkanes likely indicate variation in the degree of biodegradation of the terrigenous organic matter during original coal deposition. The variable proportions of unidentified hydrocarbons (typically terpenoids) may also reflect the variety of petrogenic conditions or, perhaps, the rank of coals in the combustion zone.

4.4. Remote sensing applications to emission estimates

Airborne IR imagery collected over the same period as the ground-based measurements was used to estimate CO_2 emissions from the Ankney and Welch Ranch fires; results for the Welch Ranch fire were previously presented in Engle et al. (2011). As described in Section 3.4, the thermal data were reduced to a land signal, a water signal (constant at this scale), and a fire signal. The most intense fire signal at Ankney was confined to a relatively small, arcuate area, representing the fire front as of May 2009 (Fig. 8). For the 0.28 ha active fire area, the total heat emission was determined to be 0.68 ± 0.042 MW. For comparison, the Welch Ranch fire, described by Engle et al. (2011), was emitting 0.48 ± 0.20 MW of total heat over

Table 4
Methane, carbon monoxide, carbon dioxide, carbon–sulfur compounds and a suite of organic compounds in exhaust gas samples. $<dl$ = less than method detection limit.

Common name	Formula	Concentration[a]	Hotchkiss		Welch Ranch		Ankney			
			Vent 5	Vent 8	Vent 1	Vent 10	Vent 3	Vent 6	Vent 7	Vent 9
Carbon dioxide	CO_2	ppmv	22,400	34,700	40,400	11,900	5780	12,300	24,600	179,000
Carbon monoxide	CO	ppbv	102	149	236	246,000	5780	56,000	74,700	344,000
Carbonyl sulfide	OCS	pptv	725	4880	4990	93,300	12,700	4080	16,300	407,000
Dimethyl sulfide	$S(CH_3)_2$	pptv	$<dl$	$<dl$	$<dl$	157	168	$<dl$	$<dl$	599
Carbon disulfide	CS_2	pptv	$<dl$	20	111	1400	225	85	179	18,400
Aliphatic Compounds										
Methane	CH_4	ppmv	610	873	127	471	609	60.3	535	7410
Ethane	C_2H_6	pptv	29,700	1,260,000	627,000	18,100,000	2,060,000	479,000	770,000	962,000
Ethene	C_2H_4	pptv	621	35,800	34,700	1,250,000	1,370,000	28,200	574,000	1,050,000
Ethyne	C_2H_2	pptv	213	657	1240	14,600	2300	1100	30,800	1,050,000
Propane	C_3H_8	pptv	314	136,000	44,600	4,240,000	448,000	34,200	127,000	41,200
Propene	C_3H_6	pptv	20.5	6320	3180	826,000	468,000	2370	114,000	167,000
i-Butane	C_4H_{10}	pptv	36,700	180,000	37,800	459,000	430,000	28,700	9330	24,100
n-Butane	C_4H_{10}	pptv	262	27,000	6100	784,000	96,900	4650	18,500	3320
trans-2-Butene	C_4H_8	pptv	1130	1390	292	137,000	67,000	256	1130	5330
cis-2-Butene	C_4H_8	pptv	657	379	134	76,400	38,700	106	774	3660
i-Butene	C_4H_8	pptv	316	2000	298	112,000	62,300	115	1700	32,700
1-Butene	C_4H_8	pptv	268	1410	151	65,000	13,200	141	672	7150
i-Pentane	C_5H_{12}	pptv	28,100	120,000	21,900	260,000	345,000	16,800	3930	3990
n-Pentane	C_5H_{12}	pptv	607	14,300	4010	223,000	26,900	3750	5760	537
n-Hexane	C_6H_{14}	pptv	152	4180	1650	158,000	12,800	1120	1870	179
2,3-Dimethylbutane	C_6H_{14}	pptv	4730	13,900	1670	7170	24,300	1200	108	60.1
2-Methylpentane	C_6H_{14}	pptv	2970	34,000	6620	103,000	86,800	5920	5560	482
3-Methylpentane	C_6H_{14}	pptv	1600	14,000	2630	23,900	42,600	1900	245	1670
Cyclohexane	C_6H_{12}	pptv	47.1	3030	518	51,500	10,500	361	675	55.3
Methylcyclopentane	C_6H_{12}	pptv	52.4	1630	247	2760	9110	111	$<dl$	34.0
n-Heptane	C_7H_{16}	pptv	66.0	879	1410	108,000	10,300	475	1330	424
2,4-Dimethylpentane	C_7H_{16}	pptv	1010	12,700	1640	53,900	58,700	1130	310	102
2,3-Dimethylpentane	C_7H_{16}	pptv	219	1030	263	8850	10,200	177	$<dl$	$<dl$
2-Methylhexane	C_7H_{16}	pptv	354	4900	935	14,400	31,700	771	111	567
3-Methylhexane	C_7H_{16}	pptv	219	1090	433	16,900	24,000	321	58	380
n-Octane	C_8H_{18}	pptv	71.7	1890	2100	62,400	5510	1630	787	162
2,2,4-Trimethylpentane	C_8H_{18}	pptv	2650	9380	2450	5980	7060	605	$<dl$	640
n-Nonane	C_9H_{20}	pptv	168	133	5090	36,800	3700	3780	955	24.8
Aromatic Compounds										
Benzene	C_6H_6	pptv	2770	3200	6590	1,750,000	3,060,000	4900	159,000	3,810,000
Toluene	C_7H_8	pptv	920	1430	12,200	489,000	176,000	9530	7940	20,300
Ethylbenzene	C_8H_{10}	pptv	167	400	3630	35,300	23,600	2870	1010	817
m&p-Xylene	C_8H_{10}	pptv	491	1740	7490	101,000	86,300	6220	3560	898
o-Xylene	C_8H_{10}	pptv	383	692	7230	44,700	27,000	5950	1600	389

[a] ppmv = 1 part in 10^6; ppbv = 1 part in 10^9; pptv = 1 part 10^{12}.

an area of 0.78 ha. Normalized for the relative areas, Ankney, therefore, had a heat flux 3.9 times that of Welch Ranch. As such, the Ankney burn was considerably more vigorous than that of the Welch Ranch fire. Extrapolating from the estimated amount of coal combusted per day at Welch Ranch and assuming complete conversion of carbon to CO_2 (examining dominant carbon-bearing gases in vent measurements [CO_2, CO, and CH_4], 94% of the carbon measured in vents was emitted as CO_2), and that the heating value of the coal at Ankney is the same as that for the Welch Ranch fire, the Ankney

Table 5
Coal-fire related minerals collected from the Welch Ranch fire by G.B. Stracher during an earlier trip in 2004. With the exception of the sulfur, inferred to be present based on appearance, all minerals were identified by X-ray diffraction.

Latitude	Longitude	Collection area	Sample color	Mineral X-ray identification	Depositional substrate of mineral(s)*
44°56′ 24″N	106°57′ 56″W	Surface hot spot	White/ yellow	Gypsum, sulfur (?)	Red clinker[a]
44°56′ 23″N	106°57′ 59″W	Gas vent	White	Tschermagite, quartz	Red clinker
44°56′ 23″N	106°57′ 59″W	Gas vent	White	Cristobalite, quartz	Red clinker

[a] Red clinker is primarily composed of baked shale.

heat flux indicates an estimated combustion of 6.4–13.8 t coal/d and 12.9–27.1 t CO_2/d.

4.5. Rate of fire advancement to estimate CO_2 emissions

Data on the rate of fire advance, i.e. coal consumption, for the Ankney fire allowed for a gross method to estimate CO_2 emissions. The maximum extent of the fire was mapped during several campaigns from May 2004 to September 2011; over that period the surface disturbed by the Ankney fire grew from 0.6 to 1.4 ha (Fig. 3). There are no drill holes adjacent to the fire, but the well log for a nearby coal bed methane well (0.4-km away) shows an 8 m thick coal bed at about the same elevation as the burning coal bed. Based on the increase in the area burned and assuming the 8 m coal thickness, about 80,800 tons of coal would have been burned, equal to 30 t/d over the previous 7 years. This is 3- to 6-times higher than the estimated combustion rate calculated for the Ankney fire in May 2009 based on the airborne IR data, assuming that the entire thickness of the coal bed burned.

5. Discussion

Comparison of gas chemistry, gas flow, and tar composition indicates that obvious differences exist both across individual fires and

Table 6

Organic composition of tar samples collected from vents at the Hotchkiss and Welch Ranch coal fires. Degree of pyrogenic weathering defined via: Light — N0>P0; Moderate — N0<P0>PY0.

Compound		Hotchkiss coal fire				Welch Ranch coal fire			
	Sample ID:	HV01-B #3	HV05 #2	HV07 #2	HV08 #2	WV12 #1	WV12 #3	WV12 #6	WV12 #7
	Source:	Vent 1	Vent 5	Vent 7	Vent 8	Vent 1	Vent 3	Vent 6	Vent 7
Total Extractable Hydrocarbons (TEH; C9-C44)	mg/kg	216,000	205,000	108,000	54,600	124,000	89,500	1,000,000	901,000
EPA PAHs:									
Napthalene (N0)	mg/kg	9.23	18.8	4.19	3.88	9.60	24.8	101	44.7
Acenaphthylene (AY)	mg/kg	2.67	5.51	0.58	1.08	0.39	0.88	28.6	12.6
Acenaphthene (AE)	mg/kg	0.87	<4.30	0.58	0.38	0.73	0.99	15.4	<6.50
Fluorene (F0)	mg/kg	3.34	8.78	1.55	0.91	1.14	2.05	27.3	18.4
Phenanthrene (P0)	mg/kg	8.46	23.5	5.02	4.65	34.8	97.4	72.3	78.2
Anthracene (A0)	mg/kg	2.27	5.25	0.69	1.04	<0.25	0.96	14.6	13.4
Fluoranthene (FL0)	mg/kg	3.49	13.1	3.64	2.50	1.25	1.6	13.7	32.8
Pyrene (PY0)	mg/kg	4.20	13.3	3.80	2.65	1.26	1.54	16.9	31.6
Benzo[a]anthracene (BA0)	mg/kg	2.64	6.20	1.47	1.16	0.27	0.72	13.1	8.59
Chrysene (C0)	mg/kg	3.62	12.7	2.59	2.22	0.73	1.86	21.5	28.1
Benzo[b]fluoranthene (BBF)	mg/kg	3.09	9.05	2.34	2.15	0.63	0.92	18.5	11.5
Benzo[k]fluoranthene (BJKF)	mg/kg	3.71	7.72	1.52	1.85	0.60	0.86	22.6	9.54
Benzo[a]pyrene (BAP)	mg/kg	3.64	6.04	1.97	2.08	0.88	0.66	27.9	15.4
Indeno[1,2,3-cd]pyrene (IND)	mg/kg	4.59	8.64	1.63	1.92	0.53	1.05	19.0	10.8
Dibenz[a,h]anthracene (DA)	mg/kg	6.46	6.28	0.90	1.20	0.21	0.45	5.94	3.84
Benzo[g,h,i]perylene (GHI)	mg/kg	4.38	7.45	2.02	1.86	0.60	1.05	19.6	10.3
Sum of EPA PAHs:	mg/kg	66.7	152–157	34.5	31.5	53.6–53.8	138	438	330–336
EPA PAHs/TEH	%	0.031	0.074–0.076	0.032	0.058	0.043	0.154	0.038	0.037–0.038
FL0/PY0	Unitless	0.83	0.98	0.96	0.94	0.99	1.04	0.81	1.04
(BBF+BJKF)/BAP	Unitless	1.87	2.78	1.96	1.92	1.40	2.68	1.47	1.37
Degree of pyrogenic weathering (PWI)		Light	Moderate	Moderate	Moderate	Moderate	Moderate	Light	Moderate

among the three fires. In the case of the former, the most striking example is that of the Welch Ranch Fire where the vents align along a linear northwest–southeast trend (Fig. 4B) with a corresponding

decrease in surface elevation towards the Tongue River (Fig. 9). Carbon monoxide, H_2S, and CH_4 concentrations increase from below detection limits at the upland vents (1–6) to elevated levels in the
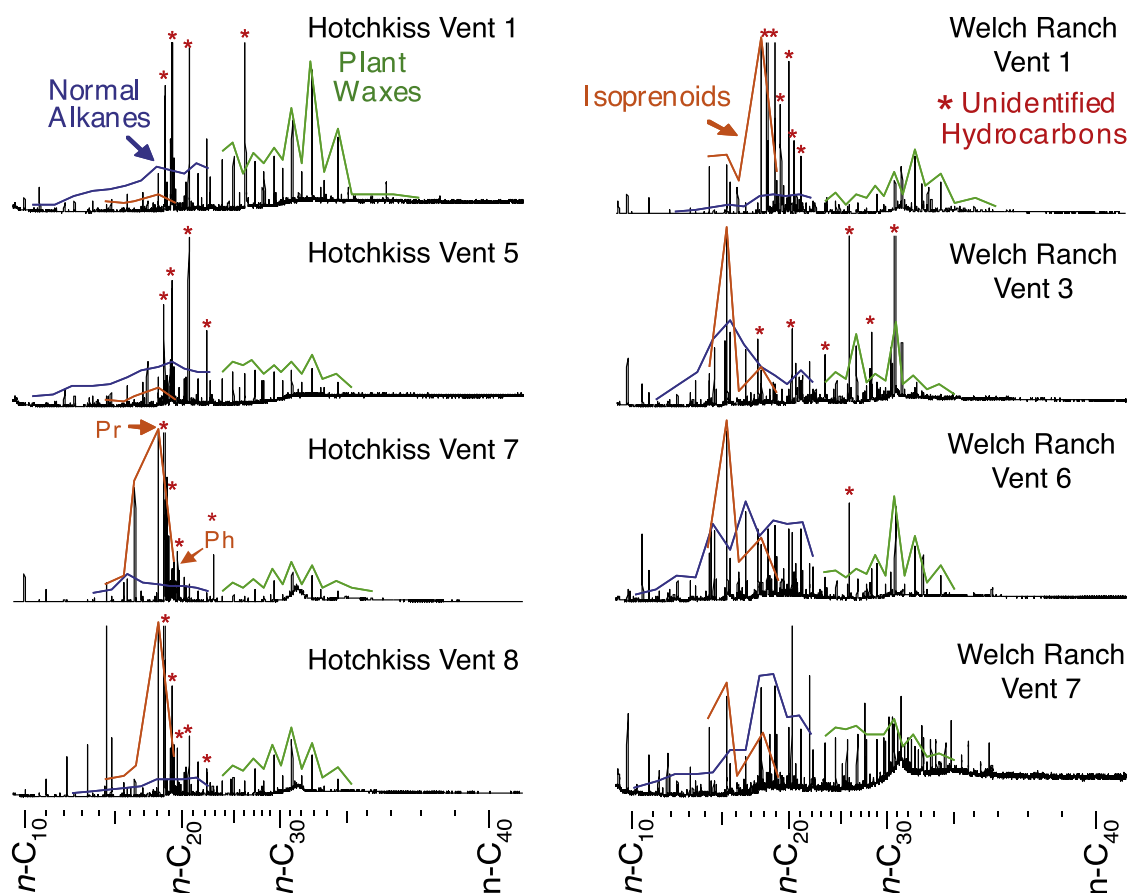

Fig. 7. GC-FID chromatograms of total extractable petroleum hydrocarbons from tar samples collected from vents at the Hotchkiss and Welch Ranch coal fires. Some peaks left unidentified due to lack of confidence in matches with compounds in the data library. Pr = pristane; Ph = phytane.
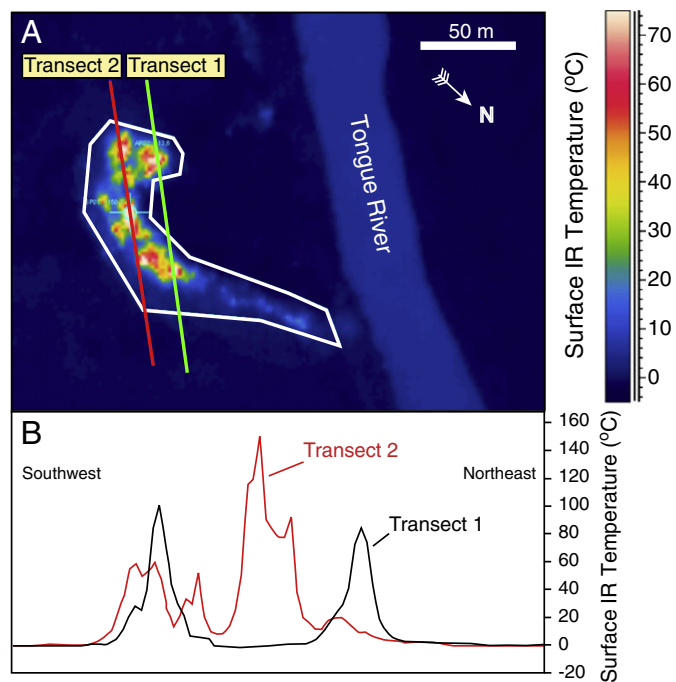
Fig. 8. (A) False color airborne thermal IR image of the Ankney coal fire. The active fire is within the arcuate area to the left of the river. The white polygon delineates the boundary around the fire-related temperature anomaly. (B) The surface IR temperature profile along two transects across the fire. At this scale, the temperature peaks at 150 °C, along Transect 2.

vents at lower elevation (Table 2). Similarly, concentrations of aliphatic and aromatic compounds in samples of exhaust gas are considerably higher, by at least one to two orders of magnitude, at vent 10 vs. vent 1. Tars collected from vents 6 and 7 contain substantially higher concentrations of TEH relative to those from vents 1 and 2 (Table 6) and also show a notable increase in unresolved compounds in GC-FID chromatograms (i.e., a development of a positive mound in the baseline) in carbon numbers 20–40 (Fig. 7). All of these independent lines of evidence suggest that a spatial variation in combustion efficiency was present at the Welch Ranch fire during the sampling campaign. Using the CO_2/CO ratio as an indicator for combustion completeness, a pattern with vent surface elevation is evident (Fig. 9).

A second possible explanatory parameter, vent temperature, was also investigated, but Mann–Whitney U tests indicate no significant difference in exhaust gas temperature between the vents 1–7 and vents 8–12 ($p > 0.05$).

We propose two possible explanations for the variance in vent gas and tar composition along the elevation trend. The first explanation pertains to the fact that there are at least two coals burning at the Welch Ranch site (Fig. 9). Higher concentrations of rapidly depositing species, e.g. H_2S, in the lower elevation vents suggest that the lower coalbed, the Dietz 3 coal, has a fairly direct conduit to the vents on the slope closer to the Tongue River. The burning of the Dietz 3 coal may be heating the upper coal, the Dietz 2 coal, dewatering and otherwise, to some extent, devolatilizing the coal. In this case, CO_2 in vents 1–6 could be derived either from combustion of the upper coal or advection and diffusion through the upper coal of gas emitted from the lower coal. Ultimately, the heating and drying, possibly augmented by repeated wetting and drying cycles, of the upper (Dietz 2) coal would result in its combustion, but at a burn front offset from the lower (Dietz 3) coal. A second explanation for the observed variation in combustion efficiency is that more complete combustion occurs on the upwind, upslope portion of the site, and efficiency decreases toward the downwind portion of the site, closer to the river. Assuming that the dominant subsurface direction of airflow in the fire also moves in the same direction, lower combustion efficiency in the lower elevation vents (i.e., vents 9–12) may be a result of upgradient oxygen depletion leading to O_2-poor conditions near the end of a subsurface flowpath.

The Hotchkiss, Welch Ranch, and Ankney coal fires emit large quantities of CO_2; volatile toxic, mutagenic, and carcinogenic organic species; and Hg. We have noted for coal fires elsewhere (Hower et al., 2009; O'Keefe et al., 2010), that combustion is less complete compared with the combustion that occurs in coal-fired utility power plants. However, unlike the power plant environment, the emissions from a coal fire are uncontrolled. Additionally, Hg concentrations in vents at the Ankney fire suggest that coal fires may be an important source of atmospheric Hg, at least locally, especially when considering the number of coal fires (thousands) thought to exist internationally.

As more coal-fire emission data are generated, comparison of emissions and fluxes should provide insight into natural, spatial, and temporal variability and data scalability. The CO_2 emission estimates from airborne remote sensing and estimation of fire advancement
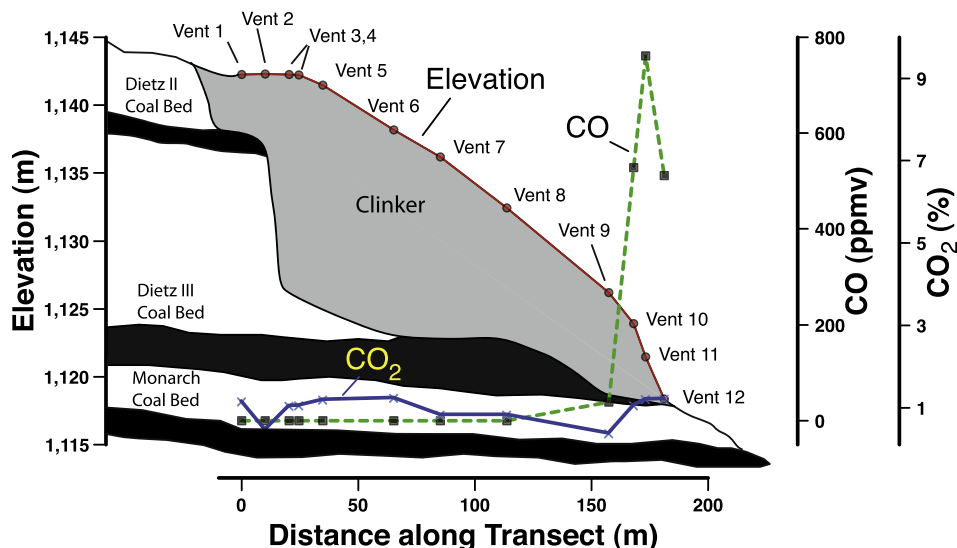

Fig. 9. Cross-section from vent 1 to vent 12 at the Welch Ranch fire (see Fig. 5b for vent locations) showing surface elevation and CO and CO_2 concentrations of exhaust gases (May 13, 2009 data). Also shown: idealized geologic cross section of the site based on field data, after Murja (2002).

Table 7
Comparison of CO_2 emission estimates for the Hotchkiss, Welch Ranch, and Ankney coal fires. ND = not determined.

Fire	Ground-based data			Airborne data total	Rate of fire advancement total	Data source
	Diffuse t CO_2/day	Vent t CO_2/day	Total t CO_2/day	t CO_2/day	t CO_2/day	
Hotchkiss	4.0 ± 0.48	ND	>3.5–4.5	ND	ND	This study
Welch Ranch	1.2 ± 0.2	6.7 ± 0.9	6.8–9.0	3.5-4.1	ND	Engle et al. (2011)
Ankney	>0.91 ± 0.24	>1.6 ± 0.09	>2.2–2.8	12.9-27.1	36–80	This study

methods indicate that the Ankney fire emits up to 80 t/d, roughly 1.5 to 20 times more CO_2 than either of the other two fires (Table 7). For comparison, a 514-MW coal-fired boiler in Eastern Kentucky produces >1000 t CO_2/d and roughly 100 g Hg/d (Center for Global Development, 2007; O'Keefe et al., 2010). Normalizing the emissions to the area of each fire, i.e. flux, there is a nearly a 3-order of magnitude variation in CO_2 fluxes between sites, despite their close proximity and the similarity in the coal composition (Table 8). These differences highlight variations in the rate at which the different fires consume coal. Our flux data indicate that the Ankney fire was consuming coal ~10–100 times faster than Welch Ranch fire and ~25–750 times faster than the Hotchkiss fire. These results also generally follow the difference in temperatures measured at the fires; the hottest fire, i.e. the fire consuming the most coal, produces the largest flux of gases. By comparison, a gob pile fire near Mulga, Alabama, exhibited a CO_2 flux on the low end of estimates for the Ankney fire. Given surface features, temperatures, and the estimated fire intensity, our estimates of total CO_2 flux for the fires correspond well with average CO_2 equivalent fluxes for coal mine spoil piles in Australia under varying degrees of combustion (Carras et al., 2009). The flux estimates compiled in Table 8 may serve as a first step in providing a range of possible values for coal-fire CO_2 emissions for national and international inventories.

One major caveat to the potential extrapolation of coal-fire emission estimates is the impact of temporal variability. As discussed previously in this paper, vent CO_2 emissions at the Welch Ranch fire decreased by ~50% in measurement sets collected within 48 h. Finer resolution time series data presented by Hower et al. (2011) demonstrate that the concentrations of coal-fire gases vary substantially within daily and hourly time scales. The impact of temporal variability in fires has important implications for scaling emission estimates to longer time scales and is currently being investigated further.

The composition and potential mobility of the tar samples and the compounds that comprise them show that gaseous emissions are not the only potential mechanism for release of coal-fire contaminants into the environment. Querol et al. (2011) examined the leachability of inorganic elements from coal-fire tars and minerals and found that freshly formed samples produced acid (pH 1.6–4) solutions, capable of dissolving trace elements. However it is unclear how general these results are to other fires and environments. The availability and transport of organics from coal-fire tars are much less well known and require further study.

6. Summary

Ground-based surveys of three coal fires and airborne surveys of two of the fires in the Wyoming portion of the Powder River Basin were conducted in May 2009. The Hotchkiss fire has the lowest coal consumption rate per area (based on total CO_2 flux of 0.9–1.1 mg/s/m²) releasing roughly 4.0 t CO_2/d through diffuse soil emissions. Hotchkiss vent gases contained the highest CO_2 concentrations of any vent in the study (3.06%) and the lowest Hg concentrations (mean = 58 ng/m³). The composition of exhaust gas and tar chemistry at the Welch Ranch fire varied along a transect parallel to the vents. Results show that combustion efficiency, i.e. higher CO_2/CO and lower relative abundance of aromatics, is greater in gases in the high elevation vents and decreases with elevation, closer to the river. We suggest the following explanations for this trend: 1) chemical variations between the two burning coal beds; and 2) consumption and decrease in O_2 along the subterranean flow path. The estimated total CO_2 flux for the fire (1.9–6.0 mg/s/m²) was similar to that of non-venting coal mine spoil piles in Australia. The Ankney fire burns more intensely than the two other fires (CO_2 flux = 25–780 mg/s/m²). Ground-based measurements over portions of the fire indicate Hg concentrations in vents exceeded background ambient air concentrations by up to ~4 orders of magnitude (12,100 ng/m³) and benzene concentrations ranged up to 3.81 ppmv.

The emissions and concentrations of CO, CO_2, volatile gases, such as benzene, and volatile metal species, primarily Hg, are at levels that may be of potential human health and environmental concern near all three of the fires. The amount of coal being consumed by the fires is less than at a coal-fired power plant, but, in contrast to the latter setting, the natural coal fires do not necessarily represent complete combustion and the emissions from natural fires are uncontrolled. While sizable strides on investigating the products of coal fires have occurred in the last several years, more research is required to adequately assess and understand the role of coal fires with respect to emission inventories and human and environmental health.

Table 8
Summary and comparison of total CO_2 fluxes for coal fires in the United States and Australia.

Fire	Area (ha)	Total CO_2 flux (mg/s/m²)	Estimate type	Notes	Coal rank	Source
Hotchkiss, Wyoming USA	4.7	0.90–1.1	Diffuse only	Mine fire	Subbituminous	This study
Welch Ranch, Wyoming, USA	1.7	1.9–6.0	Airborne and ground-based	Mine fire	Subbituminous	Engle et al. (2011)
Ankney, Wyoming, USA	0.58	25–780	Airborne and rate of fire advance	Outcrop fire	Subbituminous	This study
North, Colorado, USA	~5.3	0.28–0.51	Subsidence rate, chimney modeling, and ground-based	Outcrop fire	High volatile bituminous (?)	Ide and Orr (2011)
Mulga, Alabama, USA	9.1	27–48	Diffuse only	Gob pile fire	Low volatile bituminous	Engle et al. (2011)
Combusting coal mine spoil with active gas venting	–	260 ± 290[a]	Diffuse only	–	Bituminous	Carras et al. (2009)
Combusting coal mine spoil with no signs of venting	–	3.0 ± 4.1[a]	Diffuse only	–	Bituminous	Carras et al. (2009)
Coal mine spoil with no signs combustion	–	0.4 ± 0.6[a]	Diffuse only	–	Bituminous	Carras et al. (2009)

[a] Sum of diffuse CO_2 and CH_4, in terms of equivalent CO_2 greenhouse impact.

Disclaimer

Acknowledgments

References

Barletta B, Meinardi S, Simpson IJ, Zou S, Sherwood Rowland F, Blake DR. Ambient mixing ratios of nonmethane hydrocarbons (NMHCs) in two major urban centers of the Pearl River delta (PRD) region: Guangzhou and Dongguan. Atmos Environ 2008;42:4393–408.

Bergfeld D, Evans WC, Howle JF, Farrar CD. Carbon dioxide emissions from vegetation-kill zones around the resurgent dome of Long Valley caldera, eastern California, USA. J Volcanol Geoth Res 2006;152:140–56.

Bragg LJ, Oman JK, Tewalt SJ, Oman CJ, Rega NH, Washington PM, et al. U.S. Geological Survey coal quality (COALQUAL) database: version 2.0. U.S. Geological Survey Open File Report 97–134; 1997.

Carras JN, Day SJ, Saghafi A, Williams DJ. Greenhouse gas emissions from low-temperature oxidation and spontaneous combustion at open-cut coal mines in Australia. Int J Coal Geol 2009;78:161–8.

Center for Global Development. Carbon monitoring for action CO_2 emission database. http://carma.org/2007. accessed 9 April 2009.

Colman JJ, Swanson AL, Meinardi S, Sive BC, Blake DR, Rowland FS. Description of the analysis of a wide range of volatile organic compounds in whole air samples collected during PEM-tropics A and B. Anal Chem 2001;73:3723–31.

Dunrud CR, Osterwald FW. Effects of coal mine subsidence in the Sheridan, Wyoming, area: U.S. Geological Survey Professional Paper 1164; 1980. 49 pp.

Engle MA, Gustin MS, Goff F, Counce DA, Janik CJ, Bergfeld D, et al. Atmospheric mercury emissions from substrates and fumaroles associated with three hydrothermal systems in the western United States. J Geophys Res 2006;111: D17304. doi:10.1029/2005JD006563.

Engle MA, Radke LF, Heffern EL, O'Keefe JMK, Smeltzer CD, Hower JC, et al. Quantifying greenhouse gas emissions from coal fires using airborne and ground-based methods. Int J Coal Geol 2011;88:147–51.

Engle MA, Olea RA, Hower JC, Stracher GB, Kolker A. Methods to quantify diffuse CO_2 emissions from coal fires using unevenly distributed flux data. In: Stracher GB, Prakash A, Sokol, EV, editors. Coal and Peat Fires: A Global Perspective, Volume 2. Amsterdam: Elsevier; in press.

Heffern EL, Coates DA. Geologic history of natural coal-bed fires, Powder River basin, USA. Int J Coal Geol 2004;59:25–47.

Heffern EL, Queen G, Henke K. Technical report on the Welch Ranch coal fire, Sheridan County Wyoming. Final Environmental Impact Statement for the Pittsburg and Midway Coal Mining Company coal exchange proposal. Report from U.S. Bureau of Land Management, Casper, Wyoming, Field Office publication 2003; Appendix D: D1-D28; 2003.

Hower JC, Henke K, O'Keefe JMK, Engle MA, Blake DR, Stracher GB. The Tiptop coal-mine fire, Kentucky: Preliminary investigation of the measurement of mercury and other hazardous gases from coal-fire gas vents. Int J Coal Geol 2009;80:63–7.

Hower JC, O'Keefe JMK, Henke K, Bagherieh AH. Time series analysis of CO concentrations from an Eastern Kentucky coal fire. Int J Coal Geol 2011;88:227–31.

Ide ST, Orr Jr FM. Comparison of methods to estimate the rate of CO_2 emissions and coal consumption from a coal fire near Durango, CO. Int J Coal Geol 2011;86:95-107.

Ide ST, Pollard D, Orr Jr FM. Fissure formation and subsurface subsidence in a coal bed fire. Int J Rock Mech Min 2010;47:81–93.

Murja D. Acme-Welch coal fire construction report, Wyoming Project 17G — Statewide mine fires. Unpublished report by Spectrum Engineering to Wyoming State Abandoned Mine Land Division 2002; 10 pp.

O'Keefe JMK, Henke K, Hower JC, Engle MA, Stracher GB, Stucker JD, et al. CO, CO_2, and Hg emission rates from the Truman Shepherd and Ruth Mullins coal fires, Eastern Kentucky. Sci Total Environ 2010;408:1628–33.

O'Keefe JMK, Neace ER, Lemley EW, Hower JC, Henke KR, Copley G, et al. Old Smokey coal fire, Floyd County, Kentucky: estimates of gaseous emission rates. Int J Coal Geol 2011;87:150–6.

Pone JDN, Hein KAA, Stracher GB, Annegarn HJ, Finkelman RB, Blake DR, et al. The spontaneous combustion of coal and its by-products in the Witbank and Sasolburg coalfields of South Africa. Int J Coal Geol 2007;72:124–40.

Querol X, Zhuang X, Font O, Izquierdo M, Alastuey A, Castro I, et al. Influence of soil cover on reducing the environmental impact of spontaneous coal combustion in coal waste gobs: a review and new experimental data. Int J Coal Geol 2011;85: 2-22.

Raich JW, Potter CS. Global patterns of carbon dioxide emissions from soils. Glob Biogeochem Cycles 1995;9:1-14.

Reiners P, Riihimaki C, Heffern E. Clinker geochronology, the first glacial maximum, and landscape evolution in the northern Rockies. GSA Today July 2011;21:4–9.

Remy N, Boucher A, Wu J. Applied geostatistics with SGeMS. New York: Cambridge University Press; 2009.

Riihimaki C, Reiners P, Heffern E. Climate control on Quaternary coal fires and landscape evolution, Powder River basin, Wyoming and Montana. Geol 2009;37:255–8.

Silva LFO, Oliveira MLS, Philippi V, Serra C, Dai S, Xue W, et al. Geochemistry of carbon nanotube assemblages in coal fire soot, Ruth Mullins fire, Perry County, Kentucky. Int J Coal Geol in press.

Simoneit BRT. Organic matter of the troposphere—III. Characterization and sources of petroleum and pyrogenic residues in aerosols over the western United States. Atmos Environ 1984;18:51–67.

Stout SA, Emsbo-Mattingly SD. Concentration and character of PAHs and other hydrocarbons in coals of varying rank — implications for environmental studies of soils and sediments containing particulate coal. Org Geochem 2008;39:801–19.

Stracher GB. The origin of gas-vent minerals: isochemical and mass-transfer processes. In: Stracher GB, editor. Geology of coal fires: case studies from around the worldGeological Society of America Reviews in Engineering Geology XVII; 2007. p. 91–6.

Stracher GB. The rising global interest in coal fires. Earth Mag http://www.earthmagazine.org/earth/article/383-7da-9-12010.

Stracher GB, Nolter MA, Schroeder P, McCormack J, Blake DR, Vice DH. The great Centralia mine fire: a natural laboratory for the study of coal fires. In: Pazzaglia FJ, editor. Excursions in geology and history: field trips in the Middle Atlantic StatesGeological Society of America Field Guide 8; 2006. p. 33–45.

Uhler AD, Emsbo-Mattingly SD. Environmental stability of PAH source indices in pyrogenic tars. Bull Environ Contam Toxicol 2006;76:689–96.

Yunker MB, Macdonald RW, Vingarzan R, Mitchell RH, Goyette D, Sylvestre S. PAHs in the Fraser River basin: a critical appraisal of PAH ratios as indicators of PAH source and composition. Org Geochem 2002;33:489–515.